Seismicity of the Sunda Strait: Evidence for crustal extension and volcanological implications

Hery Harjono, Michel Diament, Jacques Dubois, Michel Larue, Mudaham Taufick Zen

TECTONICS, VOL.10, NO. 1, PAGES 17-30, FEBRUARY 1991

SEISMICITY OF THE SUNDA STRAIT: EVIDENCE FOR CRUSTAL EXTENSION AND VOLCANOLOGICAL IMPLICATIONS

Hery Harjono,[1] Michel Diament,[2] Jacques Dubois,[2] and Michel Larue [3]

Laboratoire de Géophysique, Université de Paris Sud, Orsay, France

Mudaham Taufick Zen

Laboratorium Geofisika, Bandung, Indonesia

Abstract. The Sunda Strait is located in the transitional zone between two different modes of subduction: the Java frontal subduction and the Sumatra oblique subduction. This setting implies that the Sunda Strait region is a key to the understanding of the geodynamic processes involved. In order to study the shallow seismicity, a microearthquake survey was carried out in that region. Twelve stations, accurately located by the aim of satellite positionning, recorded about 300 local events in the summer 1984. From this set, 174 shallow earthquakes have been precisely located. The results of this study reveal that the crustal earthquakes in the Sunda Strait area occurs in three main areas: (1) beneath the Krakatau complex, where earthquakes are generated by double-couples and are of tectonic origin; (2) inside a graben in the western part of the strait; and (3) in a more diffused zone to the south of Sumatra. The individual and composite focal mechanisms from the events inside the strait show an extensional regime. A stress tensor, which have been deduced from the individual focal mechanisms of earthquakes of the Krakatau group shows that the tensional axis is oriented N130°E. This study confirms that the Sunda Strait is in an extensional tectonic regime as a result of the northwestward movement of the Sumatra sliver plate along the Semangko fault zone.

[1] Also at Puslitbang Geoteknologi - LIPI, Bandung.
[2] Now at Institut de Physique du Globe de Paris.
[3] Also at ORSTOM, Nouméa, Nouvelle Calédonie.

Paper number 90TC00285.
0278-7407/90/90TC-00285$10.00

INTRODUCTION

The Cenozoic collision between the Indian continent and the Eurasian plate produced the displacement of several blocks or plates eastward or southeastward [Molnar and Tapponnier, 1975; Tapponnier et al., 1982] which must be studied in order to resolve the geodynamics of the Indonesian region. The displacement of such a block along the Semangko fault was proposed by several authors [e.g., Huchon and Le Pichon, 1984; Deplus, 1987] in order to explain the origin of the trench junction in front of the Sunda Strait. Consequently, the Sunda Strait, which is also historically famous due to the presence of the Krakatau volcano, is a key area to understanding the geodynamic evolution of western Indonesia.

The tectonic evolution of the western part of Indonesia is often related to a clockwise rotation of Sumatra by 20° relative to Java with an axis of rotation lying close to the Sunda Strait during Late Cenozoic time [Ninkovich, 1976]. The opening of the Sunda strait would then be related to that rotation [e.g., Zen, 1983]. Other authors as Huchon and Le Pichon [1984] proposed that the Sunda Strait is an extensional area which results from the northwestward displacement of the southern block of Sumatra along the Semangko fault system as a consequence of oblique subduction in front of Sumatra.

Until recently, very few geological and geophysical data were available in this area. A joint French-Indonesian study of geology and geophysics was carried out from June 1983 to February 1985 in order to collect marine and field data in and around the Sunda Strait. Marine geophysical data were intensively recorded during CORINDON IX and GEOINDON I cruises of R/V Coriolis (in 1983 and in 1984) and during KRAKATAU cruise of R/V Jean Charcot (in 1985). Furthermore, fieldwork including neotectonic studies and a microearthquake survey was conducted all around the Sunda

Strait. In this paper, we present the results of the microearthquake survey.

If we consider the seismicity of the Sunda Strait area in the context of the worldwide network, the hypocenter locations are poorly constrained, especially for shallow earthquakes, because the nearest station which could control the focal depth is located about 125 km from the strait. Moreover, no focal mechanism was available in the Sunda Strait. So, we carried out the survey in the summer of 1984 in order to constrain the shallow seismicity in the Sunda Strait area, and to better define the seismologically active tectonic features and their possible extension in the Sunda Strait. Furthermore, our goal was to check if the only active volcano in that area, Krakatau, presented some seismicity of tectonic origin and in such case to determine the relationship between the possible tectonic seismicity beneath or close to the Krakatau complex and the tectonic features of the Sunda Strait.

TECTONIC SETTING

Figures 1 and 2 show the geodynamic pattern and the geological setting of the area. The main structural features are the Java and Sumatra trench system, the Semangko fault system, and the volcanic line going from Panaitan island to Sukadana through the Krakatau complex, Sebesi, Sebuku and Rajabasa.

Java-Sumatra Trench System

The Indian-Australian plate underthrusts the Eurasian plate northward beneath the Java and Sumatra islands along the Java-Sumatra trenches. The rate of convergence of the subducting plate is 7 cm/yr [Sclater and Fisher, 1974] and the directions of relative convergence, deduced from the India/Eurasia pole of the global model of Minster and Jordan [1978] are N24°E off Java and N23°E off Sumatra. More recently, Jarrard [1986] proposed that the direction of

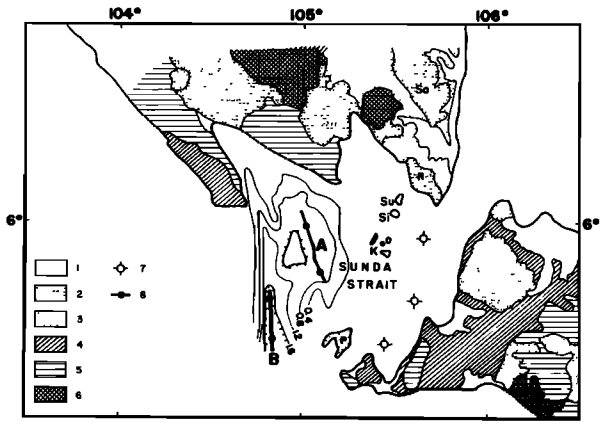

Fig. 2. Geological map of the study area simplified from Nishimura [1986]. 1, Alluvial deposit, 2, Quaternary volcanic rocks, 3, Quaternary tuff, 4, Pliocene deposit, 5, Miocene deposit, 6, Basement, 7, Locations of oil exploration drill holes, 8, Refraction profiles (A and B) of CORINDON IX. P, Panaitan island, K, Krakatau complex, Si, Sebesi volcano, Su, Sebuku volcanic island, R, Rajabasa volcano, Sa, Sukadana basalt. Simplified bathymetry (every 400m) after M.Larue (unpublished data, 1983).

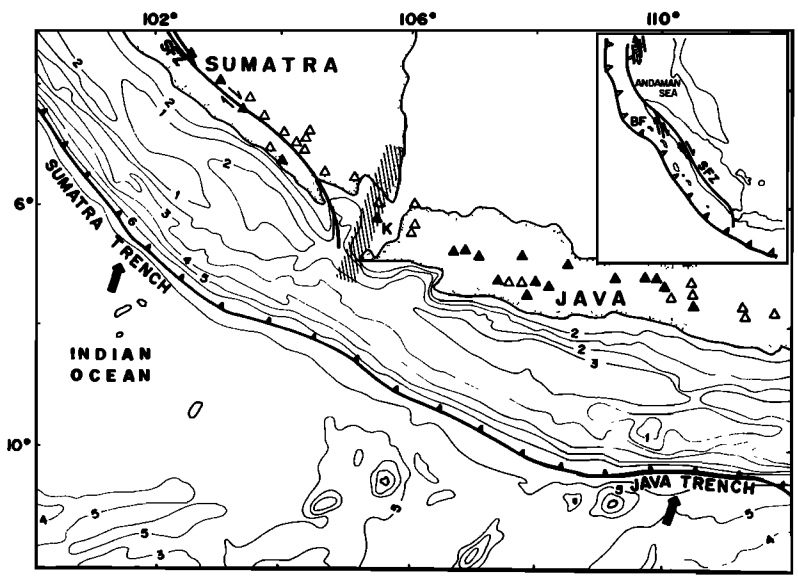

Fig. 1. Geodynamic setting of western Indonesia after Hamilton [1979]. BF is the Batee Fault. SFZ corresponds to the Semangko Fault Zone. Solid and open triangles represent active and inactive volcanoes. Hatchured zone is the volcanic line through the Krakatau complex (K). The arrows are the directions of plate convergence [after Sclater and Fisher, 1974]. Bathymetry in km.

plate convergence is nearly N-S. So, according to these directions of relative convergence and since the azimuth of the Java trench is roughly N100°E and that of Sumatra trench is N140°E, the Sunda strait area has to be considered as a transition between a frontal and an oblique subduction [Huchon and Le Pichon, 1984; Deplus, 1987].

Note that, in addition to the variation in the trench directions, the maximum depth of the Benioff zone changes, from 600 km beneath Java to 200 km beneath Sumatra [Fitch and Molnar, 1970; Hamilton, 1974; Newcomb and McCann, 1987]. Moreover, south of Java the maximum depth of the trench is greater than 6000 m, and decreases towards the Sumatra trench.

Semangko Fault System

The Semangko fault zone (Figure 1) [Van Bemmelen, 1949] runs parallel to the long axis of Sumatra and offsets right laterally the Sumatra island [Katili and Hehuwat, 1967]. According to Molnar and Tapponnier [1975], the origin of the Semangko fault is a consequence of the collision between the Indian and the Eurasian plates. The Semangko fault zone is supposed to accomodate the obliquity of the Sumatra subduction zone [Fitch, 1972; Beck, 1983; Huchon and Le Pichon, 1984].

Hamilton [1979] assumed that the fault continues southward and intersects the trench, while Huchon and Le Pichon [1984] proposed that the fault ends in the Sunda Strait as a graben. Indeed, there is no field indication that the fault extends to West Java [Nishimura et al., 1986]. However, the interpretation of gravity data from West Java indicates some trends nearly parallel to the trend of the Semangko fault [Untung and Sato, 1978]. Evidence of a NW-SE right lateral fault was recently observed during geological fieldwork in the western part of West Java (S. Pramumijoyo and M. Sébrier, personal communication, 1988). So, the question of the exact location of the active Semangko fault system is still open and can be addressed with the use of seismological data.

The Semangko fault system is also considered as the limit between the Eurasian plate and the so-called Sumatra sliver plate or forearc plate to the south [Jarrard, 1986]. In that case the Sunda Strait area would be located just to the north of a triple junction between the Indian plate, the Eurasian plate, and the Sumatra sliver plate. Furthermore, as the Sumatra sliver plate moves northwestward, the Sunda Strait area would act as a trailing edge and should present extensional structural patterns [Huchon and Le Pichon, 1984; Jarrard, 1986].

Sunda Strait

The main feature of the bathymetric pattern in the strait, according to the detailed survey of CORINDON IX in 1983 [M.Larue, unpublished data from CORINDON IX cruise, 1983], is a N-S graben with a maximum depth of about 1800 m (Figure 2). In the eastern part of the strait the sea bottom is shallower than 100 m and relatively flat; except inside the Krakatau complex, where the depths are about 200 m but are related to the calderas. The stratigraphic interpretations of seismic reflection profiles across the eastern flank of the graben clearly reveal rapid subsidence since Pliocene [Lassal et al., 1989; V.Renard et al., unpublished data from Krakatau'85 cruise, 1985]. Such rapid subsidence is also evidenced by the borehole data from an oil exploration area to the southeast of Krakatau (Figure 2) [Noujaim, 1976]. This drilling encountered a thick accumulation of Quaternary to Upper Pliocene sediment series (2450 m).

Figure 3 displays the epicenters for the period 1964-1981 as determined by the worldwide network. To obtain this figure we selected shallow earthquakes (depths less than 60 km) with magnitudes greater than 4.5 and recorded by at least 10 stations. Figure 3 reveals that the seismicity is not correlated with the bathymetry. For example, the graben is not conspicuous on Figure 3. The most pronounced figure is the N-S seismic belt which coincides with the Krakatau volcanic line. This led Nishimura et al. [1986] to interpret that seismic belt as a fracture zone. A well pronounced cluster of seismicity is also present in the south of Sumatra and seems to show a N-S linear pattern.

The area of the Sunda Strait is mostly covered by Quaternary volcanic products (Figure 2). The recent volcanic activity around the Sunda Strait occurred along the Krakatau volcanic line [Nishimura et al., 1986]. According to these authors it started in the north by alkali basaltic emplacement at Sukadana, continued to the south through Rajabasa, Sebesi, Sebuku, Panaitan, and finally ended at Krakatau. Nevertheless it must be noted that no dating has been done on Panaitan. The K-Ar age determination of the Sukadana basalt is between 0.8 and 1.2 Ma [Soeria-Atmadja et al., 1986; Nishimura et al., 1986]. Compared to the other Quaternary volcanic rocks in the region, the source of this basaltic plateau is more primitive. This might be connected to the

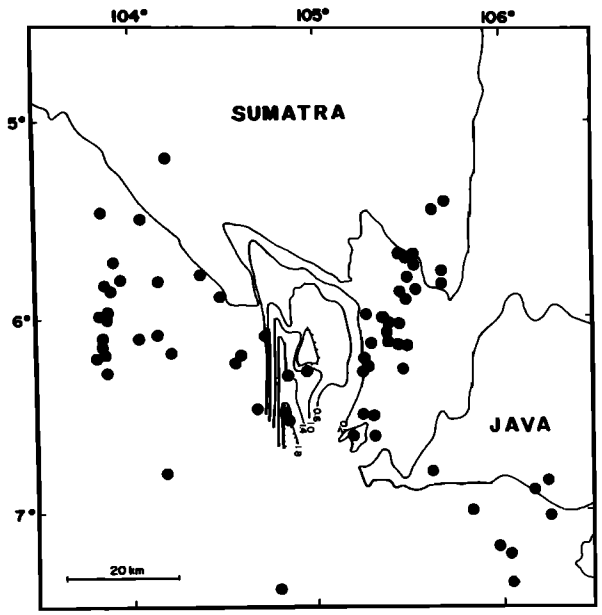

Fig. 3. Superficial (less than 60-km depth) seismicity between 1964 and 1981 as given by NEIS.

fact that the Sukadana basalt has been preferentially emplaced along NW-SE trending fractures which are subparallel to the Semangko fault system and not parallel to the Krakatau volcanic line. At present, the only active volcano in the area is the Anak Krakatau (child of Krakatau) volcano which was formed in 1927, 44 years after the famous explosion of Krakatau. According to various authors [e.g., Zen, 1983; Camus et al., 1987] Krakatau is a calc-alkaline volcano. Nevertheless petrological studies indicate some differences between the chemical compositions of the Krakatau products and those of the Java and Sumatra volcanoes nearby [Nishimura, 1986]. This would suggest that the Krakatau volcano differs from the other volcanoes in the area.

In summary, questions such as the existence of seismologically active features in the Sunda Strait, their exact locations, their relationship to the opening of the strait and their relationship to the volcanic activity and the stress regime in the area need to be studied in order to better constrain the geodynamic evolution of this region.

DATA AND ANALYSIS

Network

From July 7 to August 22, 1984, 10 portable seismographs were installed around the Sunda Strait area (Figure 4). Five of these stations (TRM, BTG, TBG, CIL, CBL) remained in operation until the end of September 1984. Two additional stations from the Volcanological Survey of Indonesia and the Geophysical and Meteorological Agency were also used in order to complete our network. The first, KRK station, is intalled on the Anak Krakatau with the signal being broadcasted to PAS station, and the second one is KLI station. All stations, except KLI, were MEQ-800 Sprengnether associated with Mark Product L4C vertical seismometer with an eigen frequency of 1Hz. KLI is a short period permanent station (Kinemetrics). The seismometer there has a peak eigen frequency of 3 Hz. The mean distance between two stations was about 30 km except for the gap between TRM and UJK in the west entrance of the Sunda Strait (Figure 4). The earthquakes were recorded either on smoked paper or with ink at a drum speed of 60 mm/min or 120 mm/min depending of the access facilities. Drift of internal clocks of all MEQ-800 was checked using WWV radio signal every 2 or 4 days. It must be noted that the drift remained linear and small, ranging from 8 ms/day to 30 ms/day. The accuracy of the clock for KLI is given by a permanent reception of WWV. The positions of the stations were located using a JMR-4 satellite receiver and, depending on the number of satellites available, were determined to an accuracy such that the resulting standard deviations were systematically smaller than 60 meters.

Hypocenter Determination

The arrival times were read using a magnifying lens and the estimated errors are of 0.1 s for the P waves and 0.5 s for the S waves. We also estimated the total amount of error on times less than twice these values especially due to the small drift of the clocks. Hypocenters were located using the Hypoinverse routine of Klein [1978].

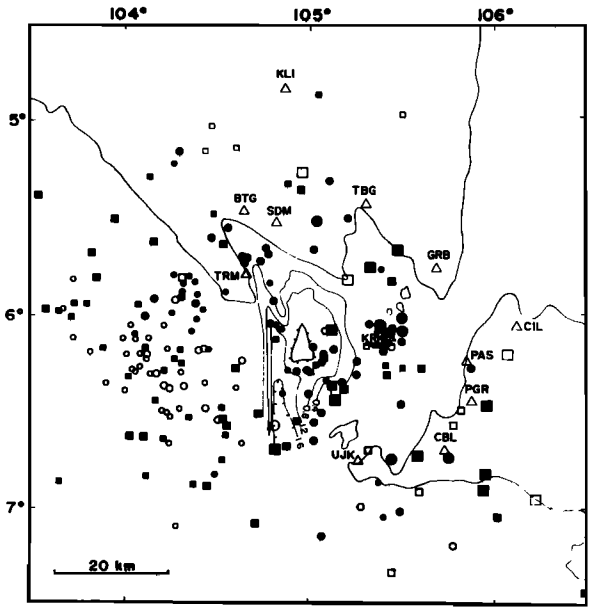

Fig. 4. All events recorded during this survey. Full and open circles correspond to the depth of 0-20 km and 20-50 km respectively. and the full and open squares correspond to 50-100 km and more than 100 km. The Krakatau area is shown with more detail on Figure 7. Size of a symbol corresponds to the class of accuracy (A, larger symbols, B, intermediate size symbols, C, smaller symbols). Triangles show the stations.

Vp/Vs ratio. The depth determination is sensitive to the choice of Vp/Vs ratio if S waves are introduced in the hypocenter calculation [McCaffrey et al., 1985]. In the present study we estimated the Vp/Vs ratio by plotting various P and S arrival times for several pairs of stations. Sixtyfive events with at least four S readings and distributed over the entire studied area were used to estimate the Vp/Vs ratio using a least squares method. The resulting value of 1.72 ± 0.01 was adopted for all other hypocenter determinations.

Crustal structure. A flat layered model was adopted for hypocenter determinations. Two seismic refraction lines were shot in the Sunda Strait during the CORINDON IX cruise [Larue, 1983]. Their locations is shown on Figure 2. Interpretation of these profiles, according to Fatwan [1983], is given in Table 1. The maximum penetration was not larger than 7 km, thus we do not have any information on the lower crust velocity structure. Therefore, the lower crust and the upper mantle velocities and the depth of the deep interfaces must be deduced from the results of tests. These tests were performed using an initial crustal model for which the depths of interfaces and the velocities were subsequently varied. We located a selected set of events (35 events a priori located inside the network) with a large number of crustal models. We then selected the most appropriate models using the mean rms [Hatzfeld et al., 1986; Kiratzi et al., 1986]. Of course the preferred crustal model strongly depends on the

TABLE 1a. Velocity Model: Profile A

Depth (km)	Vp(km/s)
0	2.6
2.2	3.1
4.9	4.0
6.8	5.7

Upper crustal model deduced from refraction data [after Fatwan, 1983]. See Figure 2 for location of profile A.

TABLE 1b. Velocity Model: Profile B

Depth (km)	Vp(km/s)
0	2.6
4.0	5.5
5.2	6.8

Upper crustal model deduced from refraction data [after Fatwan, 1983]. See Figure 2 for location of profile B.

TABLE 1c. Crustal Model Used for Determination of Hypocenters

Depth (km)	Vp(km/s)
0	3.1
4.0	5.5
9.0	6.8
22.0	7.8

See text for explanation.

starting model. For the upper crust, we adopted an average between the two interpretations of seismic refraction. For the upper mantle velocity we adopted a starting value of 8.1 km/s, a common value for this parameter. The starting Moho depth was taken from a deep refraction survey performed in the south of Java (located at lat. 8°S and long. 108.5°E) [Raitt, 1967] which gave a value of 22 km. Note that Kieckhefer [1981] used a Moho depth at 25 km and an upper mantle velocity of 8.1 km/s in order to model the results of a microseismicity network installed in the north of Sumatra to study the Semangko fault system.

As concerns the upper part, results showed that the variations of the rms remained small. This is due to the fact that most of the rays are refracted waves traveling in the lower crust. The best upper crustal model is given in Table 1c.

We then varied the Moho depth and the upper mantle velocities, the lower crust velocity and the deeper crustal interface. Results (Figures 5a and 5b) show that the best upper mantle velocity is 7.8 km/s and the one of the lower crust is 6.8 km/s. This last value is coherent with the refrac-

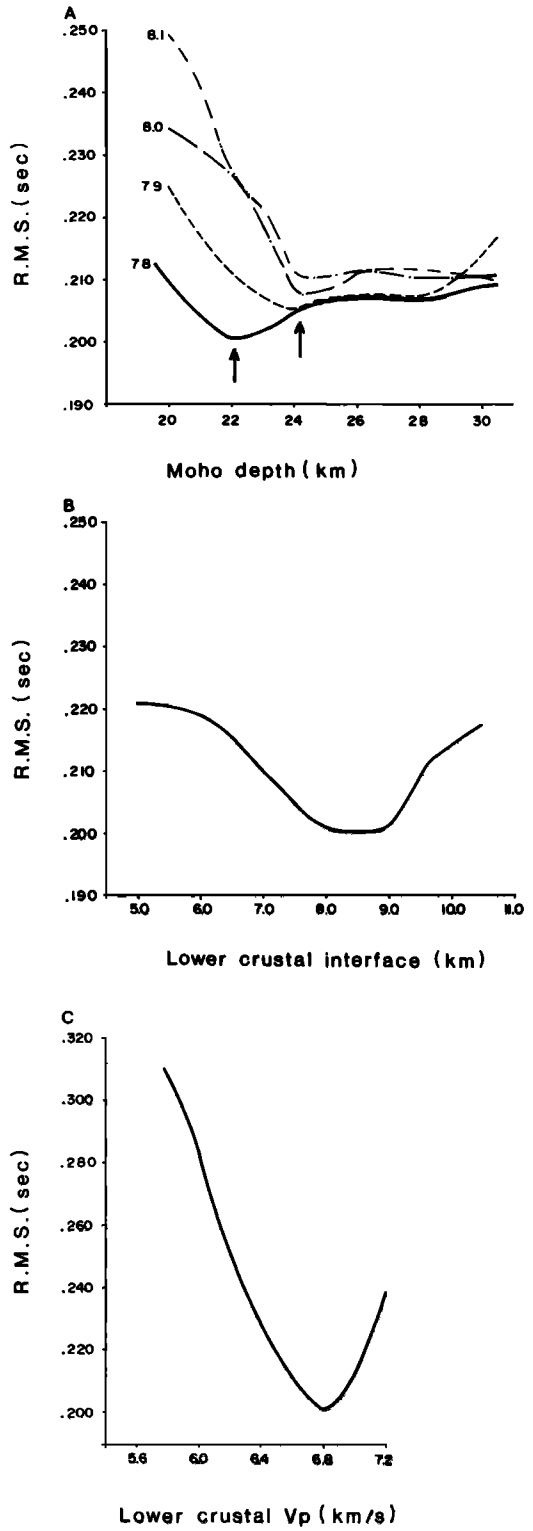

Fig. 5. (a) Variation of rms versus Moho depth and upper mantle velocity. (b) Variation of rms versus lower crustal interface. (c) Variation of rms versus lower crustal P velocity.

tion results and appears well constrained (Figure 5c). The Moho depth appears to be 22 km for the chosen upper mantle velocity and more than 24 km if a higher upper mantle velocity is taken (Figure 5a). Figure 5c shows that the lower crustal interface lies between 8 and 9 km. The resulting crustal model chosen to use for the hypocenter locations is given in Table 1c. Of course, according to these results, slightly different crustal model can be used. Therefore in the following section we will discuss the displacements of the locations according to the crustal velocity structure and to the various classes of accuracy.

Earthquake locations. We classified our hypocenters as A, B, and C depending on the criteria of statistical error and station distribution (including the number of phases used during determinations). Several tests made with 10 selected events and our average crustal model were performed in order to define our classification. We chose 10 events located inside the Krakatau complex, in the middle of the network, since the depths of these events are well controlled by the KRK station. These 10 events were first located using different sets of P arrival times (associated with S or not). In order to get an idea of the accuracy of poorly recorded events (for example, outside the network), we also relocated our test events using only readings from several limited sets of stations, for example the Sumatra stations and CIL but excluding KRK.

Results of these various tests showed that for events occuring inside the network and located using at least seven P arrival times with a distribution of stations in the four quadrants, we still got a good result, that is, the hypocenters were not shifted more than 2 km. Using six P arrival times only, the epicenters were as close as 1 km to those determined using seven arrival times but the error on the depth (ERZ) was larger (about 5 km). For events located outside the network, we had to introduce at least one S arrival time in order to obtain an acceptable accuracy (about 5 km) on the depth.

According to these results, we defined our classifications of A, B, and C events as follows. A events are those determined using at least eight phases including at least one S arrival time, with a rms less than 0.3 s, recorded by stations in at least three quadrants with at least one station with an epicentral distance (D min) less than 2 times the focal depth (2Z), and horizontal (ERH) and vertical (ERZ) error less than 5 km. B events were located using at least six phases including at least one S arrival time if outside of the network, with rms less than 0.4 s and recorded in at least two quadrants with D min less than 3Z, and ERH and ERZ less than 10 km. C class events correspond to those located using a minimum of six phases not necessarily with S, a rms less than 0.5 s, with ERH and ERZ less than 15 km. With this classification we retained only 174 shallow earthquakes among the 300 local ones recorded (Figures 4, 6 and 7).

Finally, as mentioned above, in order to quantify the quality of the locations, we investigated the displacements of the hypocenters when changing the crustal structure. For that purpose we relocated a set of randomly chosen events from classes A and B using several crustal models. These models were obtained by varying the depths of interfaces and the velocity of the lower crust with the limiting values deter-

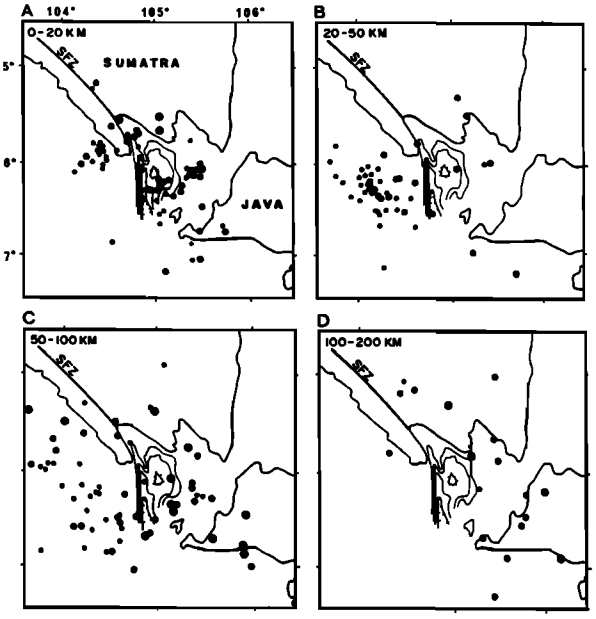

Fig. 6. Recorded seismicity as a function of depth. Size of a symbol corresponds to the class of accuracy; (larger symbols, class A, intermediate size symbol, class B, smaller symbols, class C).

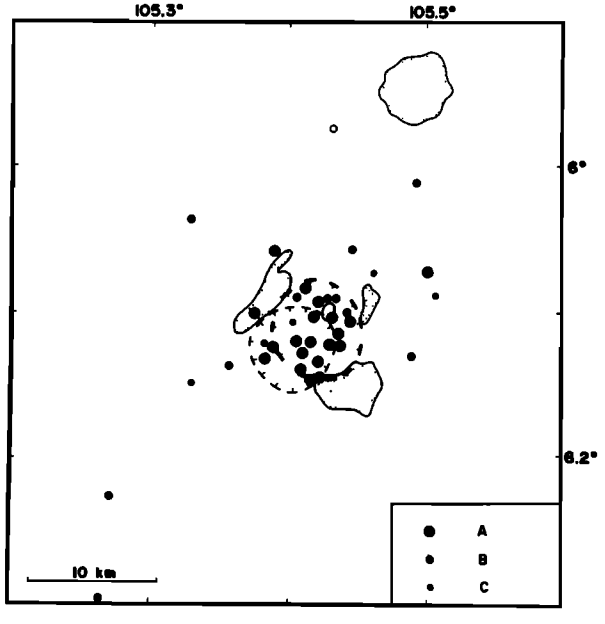

Fig. 7. Epicenters close to the Krakatau complex. Also shown are the two calderas. The thick line corresponds to the older caldera and the thin line to the one resulting from the 1883 explosion (redrawn from Camus and Vincent [1983]). Size of a symbol corresponds to the class of accuracy.

mined previously in the crustal model determination. Results show that for events A the horizontal displacement is about 1.5 km and the vertical displacement about 2.0 km, while for events B the values are 3.0 km and 5.0 km respectively.

RESULTS

Figures 4, 6 and 7 show the spatial distribution of epicenters according to the three classes. If we compare these figures with the one deduced from teleseismic network (Figure 3), we find some similarities and some differences in the seismicity patterns. We did not recorded the earthquakes forming a N20°E seismic belt that coincides with the Krakatau volcanic line as clearly shown by worldwide data. Our microearthquake data show that the events are clustered mainly beneath the Krakatau complex. Nevertheless we note that the microseismicity shown here was recorded during a very limited time period as compared to the one shown on Figure 3. On the other hand, the N-S seismicity south of Sumatra revealed on Figure 3 is clearly present in our results. Although Figure 6 shows that the shallow seismicity south of Sumatra is scattered, events seem to be roughly aligned along a N30°E-N40°E trend rather than the N-S one evidenced on Figure 3. Unfortunately that seismicity is poorly constrained since it lies outside our network.

Indeed our results reveal three very pronounced concentrations of shallow earthquakes: a Krakatau cluster, a graben cluster and a cluster south of Sumatra (Figure 6). The two first clusters are aligned along a N50°E-N60°E azimuth that roughly coincides with the southeastern flank of the graben, which is underlined by a pronounced gravity anomaly [Diament et al., 1987]. Therefore the Krakatau complex appears to lie just at the intersection of the volcanic line with a fault trending N50°E-N60°E. This probably explains why Anak Krakatau is presently the only active volcano of the volcanic line.

The northwestern flank of the graben is also underlined by a shallow seismicity that prolongates the trace of the Semangko fault zone (Figure 6). This confirms that the Semangko fault system does not cross the Sunda Strait towards Java but seems to end in the graben, as inferred by Huchon and Le Pichon [1984]. It is also noteworthy that we did not record crustal earthquakes either on Sumatra, except on the Semangko fault, or on Java. This confirms the seismicity pattern deduced from the worldwide data (Figure 3).

We discuss now the various clusters of shallow earthquakes, occuring at depths between 0 and 20 km, since we are mainly interested in the crustal seismicity.

Krakatau Cluster

Most of the events which are located beneath the Krakatau complex have been classified as A events. Figure 7 shows that the seismicity is mainly concentrated inside the Krakatau complex.

A question arises whether the events beneath this active volcano were of volcanic or tectonic origin. Earthquakes associated with a volcanic origin such as magma movements normaly have low frequencies as compared to tectonic ones. Note however that volcanic events might have an appearance of tectonic earthquakes [Minikami, 1974]. However, there is commonly evidence that the volcanic earthquakes (tremors) are not generated by a double couple [Shimizu et al., 1987] as are the tectonic ones. Concerning our data, we believe that the events beneath the Krakatau complex are of tectonic origin since they clearly showed high frequencies and all stations around the strait recorded both up and down first motions.

These earthquakes show a tight vertical distribution. Vertical cross sections from several azimuths show that they form a narrow column (Figure 8). If we consider their distribution as a function of depth, it appears that the earthquakes are concentrated between 2 and 9 km with a higher concentration in the 5-9 km range. The earthquakes are less frequent for depths greater than 10 km. The local magnitudes (magnitude duration, ML) were generally between 2.0 and 3.0. Some earthquakes located at a depth between 3 km and 8 km show magnitudes larger than 3.0; one shock even had a magnitude of 4.4.

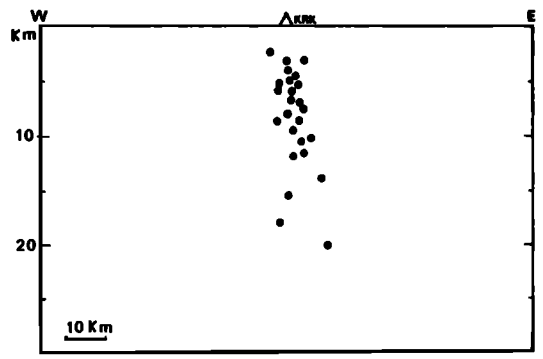

Fig. 8. East-west cross section across Krakatau.

Individual focal mechanisms of these events generally show an extensional pattern (Figures 8 and A1). However, if we consider the focal mechanisms as a function of depth, there is an apparent systematic change, from compression to extensional mechanism.

1. For depths between 0-4 km, there are only two solutions of focal mechanisms, wich both show a strike-slip with reverse components (Figure 9a).

2. Between 4 and 6 km depth, the fault plane solutions of three earthquakes (Figure 9b) show that the mechanisms are mostly controlled by extension but with some strike slip components.

3.For depths greater than 6 km, the extensional pattern seems to dominate (Figures 9c and 9d). Some earthquakes show nearly pure dip-slip. It is noteworthy that these events are located close to the flanks of the caldera (e.g., events 2, 6, 10 or 12 on Figure 9c). Thus we propose that these earthquakes correspond to displacement along faults controlled by the deep geometry of the calderas. Two events (4 and 9) in this cluster are slightly different and show solutions of lateral slip movements. Earthquake 5 located at a depth of 20 km

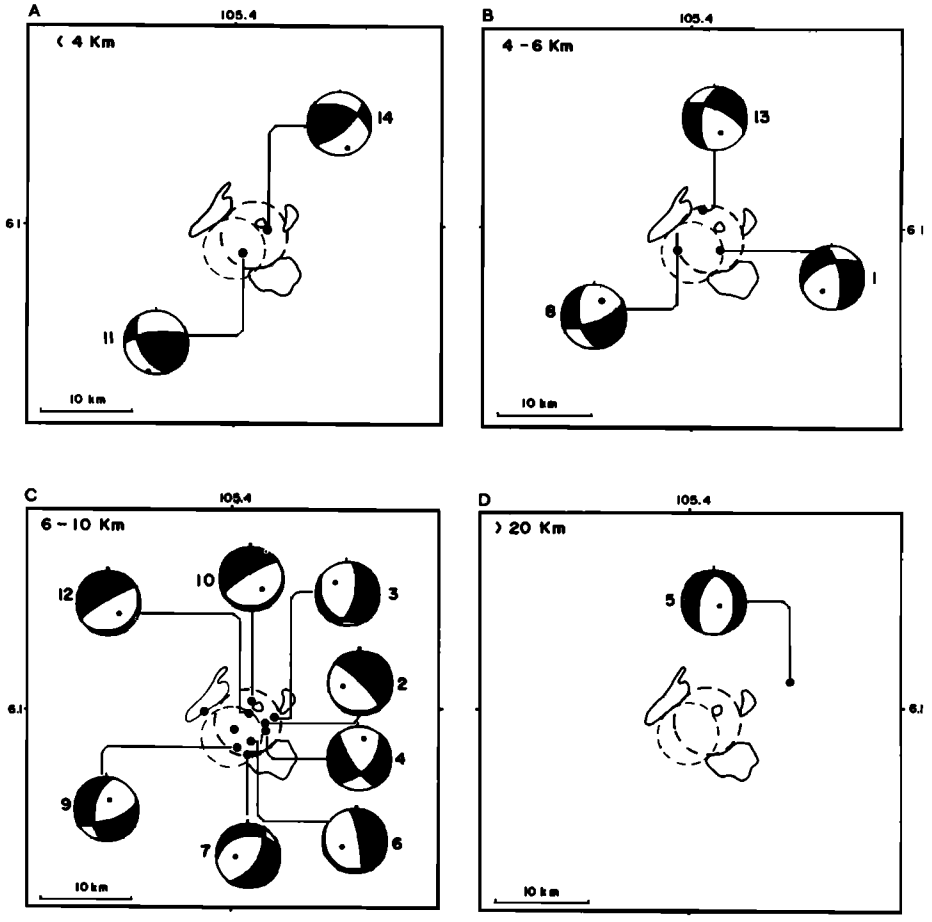

Fig. 9. Focal mechanism as a function of depth for events of the Krakatau cluster. Note the evolution from compression to extension with depth. Lower hemisphere projection and black zone correspond to compression.

shows a normal mechanism with a direction of fault plane nearly N-S (Figure 9d).

We propose that this clear variation of mechanisms with depth is related to local structural effects since the crustal structure beneath the Krakatau complex is very disturbed. Apart from the probable magma chamber, the existence of the various calderas and probable volcanic intrusions might induces local variation in the stress field.

To check this assumption of local variations we show on Figure 10 all P and T axes of events deeper than 4 km. This figure clearly confirms an extension roughly east-west for all events. We then inverted all the focal mechanisms of this set in order to obtain a stress tensor using the method of Carey-Gailhardis and Mercier [1987]. The two very shallow events with reverse faulting were not used since they significantly differ from the deeper ones and cannot be included in such a computation. Results are given in Table 2 and on Figure 11. This method allows selection of a set of preferred fault planes from a set of auxiliary planes. The preferred fault plane was chosen so that the angle between the predicted t and observed s slip vectors is small (less than about 25°) and the R value (relative ratio of principal stresses differences) is between 0 and 1 (see Carey-Gailhardis and Mercier [1987] for details). In Table 2, the preferred fault planes are underlined. The thirteen fault planes are shown on Figure 11b. $\sigma 1$, $\sigma 2$ and $\sigma 3$ are the compressional, the intermediate, and the tensional principal deviatoric stress values respectively. This computation shows that all the events are dominated by a stress regime with a N130°E extension, that is parallel to the Semangko fault. This is an indication that the stress tensor computed using only events beneath Krakatau is controlled by the regional stress regime. Finally, it appears that local variations in the stress field beneath Krakatau are such that extension takes place along more or less horizontal faults for the deepest events, along more close to the vertical ones for the 4-6 km deep events (see Table 3) and that compression dominates in the uppermost part of the crust.

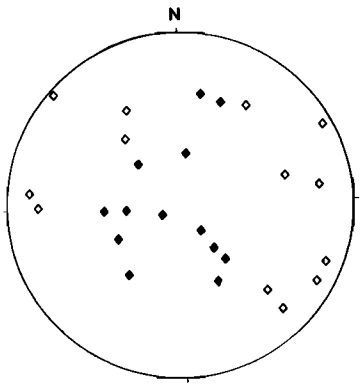

Fig. 10. Compression (solid diamonds) and tension (open diamonds) axis for the Krakatau cluster.

The Graben Cluster

Most of the events occuring in the graben are classified as B and C events. Their epicenters are clustered on the eastern flank of the graben (Figures 4, 6 and 12). There is a good correlation with the abrupt scarps in the bathymetry, either with the already mentionned southeastern flank of the graben or with the east and south flanks of the triangulary hill lying in the middle of the graben (Figures 6 and 12).

Figure 12 shows four composite focal mechanisms, which were computed using only B events. Three mechanisms show an extensional pattern. Mechanism 16 has a nearly vertical plane striking parallel to the Semangko fault. Solution 17 shows a normal fault with a strike direction nearly N-S, which agrees with bathymetric data. Although very poorly constrained (see Figure A1), mechanism 18 yields P and T axis close to the previous ones. The fourth solution, 19, gives rise to two possible interpretations as shown on Figure A1. One solution gives a T axis NW-SE and the other one is SW-NE direction. Since, as shown on Figure 13, the T axis for the graben cluster are compatible with the stress tensor determined from data of the Krakatau cluster, we can assume that the events of the graben are controlled by the same stress pattern as the ones of the Krakatau cluster. In order to discriminate the two fault plane solutions, we tested both using our tensor. One solution (shown on Figure 12) appeared to be compatible with this tensor, therefore we kept it (see Table 3).

Cluster South of Sumatra

During the survey, many earthquakes were recorded from the area south of Sumatra (Figures 4 and 6) but their magnitudes were generally small. For that reason many of the earthquakes were recorded only by the three nearest stations (BTG, SDM and TRM). Most of the events from this cluster belong to class C. As we already mentioned, this cluster is aligned approximately perpendicular to the Semangko fault. Unfortunately, we were not able to calculate focal mechanisms since the location of the earthquakes are outside the network. However, shallow earthquakes recorded by the worldwide network have been located close to this cluster. Their centroid moment tensor solutions (CMTS) [e.g., Dziewonski et al., 1989] mostly represents strike-slip faulting with an extensional component (Figure 14).

The extension direction is more or less parallel to the Semangko fault, that is, parallel to the direction of extension

TABLE 2. Computed Deviation (t,s) and R Values (see text) on the Nodal Planes of the Focal Solutions of the Krakatau Cluster

	Nodal Planes				Computed (t,s) and R Values			
	N1		N2		N1		N2	
Event	Strike	Dip	Strike	Dip	(t,s)	R	(t,s)	R
1	N356°E	68°	N241°E	50°	4.8	0.46 [a]	38.4	-1.25
2	N309°E	78°	N091°E	17°	1.2	0.42	61.7	11.62
3	N007°E	66°	N147°E	32°	59.9	1.37	12.3	0.26
4	N148°E	77°	N042°E	53°	10.8	0.50	68.4	-47.82
5	N192°E	58°	N349°E	35°	42.2	1.29	10.9	0.57
6	N345°E	82°	N151°E	8°	75.0	1.01	8.5	0.53
7	N033°E	63°	N256°E	36°	13.3	-0.50	12.9	0.09
8	N067°E	73°	N172°E	57°	11.1	0.15	27.3	-0.06
9	N195°E	30°	N066°E	70°	30.2	-0.62	4.6	0.65
10	N241°E	82°	N086°E	9°	61.2	1.03	0.3	0.33
12	N230°E	80°	N050°E	10°	30.2	1.01	0.2	0.71
13	N298°E	62°	N186°E	58°	85.0	-0.66	21.3	-0.66
15	N053°E	44°	N212°E	48°	0.6	0.08	6.9	-0.12

[a] Underlining represents preferred fault plane.

TABLE 3. Fault Plane Solutions and P, T Axes for Events of the Krakatau and the Graben Clusters

Event	Date, 1984	Time (GMT)	Lat. (°S)	Long. (°E)	Depth (km)	Mag.	Nodal Planes				P and T Axes			
							N1		N2		P		T	
							Strike	Dip	Strike	Dip	Strike	Dip	Strike	Dip
1	July 13	2104:51	6.12	105.43	5.4	2.4	N356°E	68°	N241°E	50°	N218°E	35°	N114°E	8°
2	July 23	0345:55	6.11	105.44	7.0	3.0	N309°E	78°	N 91°E	17°	N242°E	42°	N 35°E	40°
3	July 23	0354:50	6.11	105.45	7.7	3.4	N 7°E	66°	N147°E	32°	N315°E	51°	N 78°E	10°
4	July 24	1735:42	6.13	105.44	7.2	3.5	N148°E	77°	N 42°E	53°	N 10°E	24°	N270°E	10°
5	July 24	1233:28	6.08	105.50	20.3	2.9	N192°E	58°	N349°E	35°	N136°E	68°	N275°E	8°
6	Aug. 01	1030:09	6.13	105.42	9.4	3.4	N345°E	82°	N151°E	8°	N265°E	40°	N 70°E	25°
7	Aug. 01	1038:44	6.16	105.42	6.8	3.5	N 33°E	63°	N256°E	36°	N260°E	52°	N138°E	15°
8	Aug. 03	0545:51	6.12	105.40	5.5	4.4	N 67°E	73°	N172°E	57°	N 22°E	22°	N120°E	8°
9	Aug. 03	0934:37	6.14	105.41	8.2	2.8	N195°E	30°	N 66°E	70°	N 12°E	58°	N138°E	30°
10	Aug. 04	1150:28	6.09	105.42	6.1	1.9	N241°E	82°	N 86°E	9°	N138°E	42°	N330°E	45°
11	Aug. 06	0115:26	6.13	105.41	3.4	3.4	N150°E	53°	N265°E	65°	N205°E	5°	N120°E	40°
12	Aug. 13	1415:41	6.10	105.42	6.8	2.2	N230°E	80°	N 50°E	10°	N138°E	52°	N330°E	45°
13	Aug. 13	1733:38	6.08	105.41	4.9	3.4	N298°E	62°	N186°E	58°	N151°E	35°	N320°E	35°
14	Aug. 13	1755:35	6.07	105.43	3.4	2.5	N 49°E	68°	N290°E	44°	N162°E	10°	N270°E	40°
15	Aug. 30	1507:32	6.10	105.40	8.8	2.2	N 53°E	44°	N212°E	48°	N236°E	72°	N315°E	2°
16	Composite						N320°E	80°	N217°E	47°	N200°E	38°	N 82°E	28°
17	Composite						N176°E	59°	N347°E	42°	N138°E	40°	N265°E	10°
18	Composite						N195°E	79°	N318°E	24°	N108°E	70°	N275°E	20°
19	Composite						N235°E	65°	N 52°E	26°	N154°E	65°	N325°E	20°

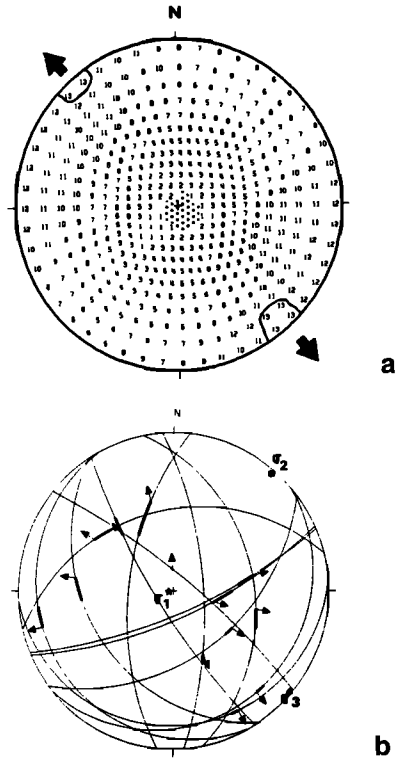

Fig. 11. (a) Superimposition of the tensional right dihedra of the 13 focal mechanisms of the Krakatau cluster showing a N130°E extension. The tensional zone is defined by area containing the number 13. The compression is shown by the dotted area, i.e. subvertical. (b) Deduced seismic fault planes and principal axis of the computed stress tensor. Arrows denote computed slip on the faults. See text for further explanation.

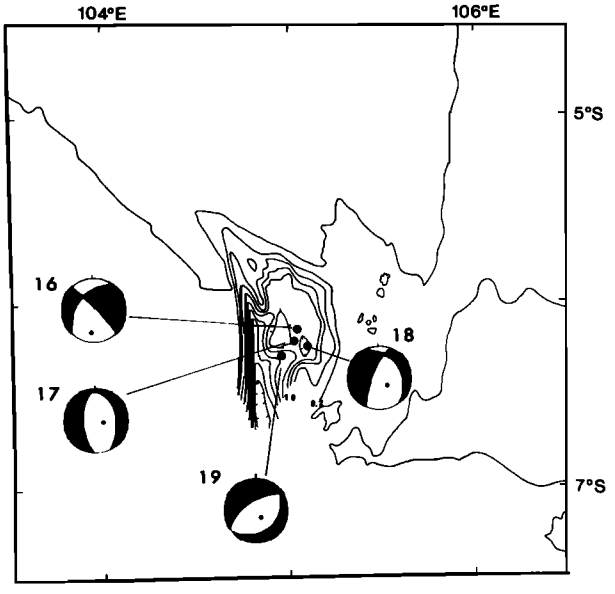

Fig. 12. Composite focal mechanisms for some selected events of the graben cluster. Composites were computed using closely located earthquakes with identical depth.

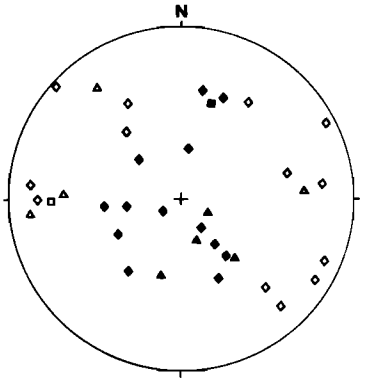

Fig. 13. P and T axis for all events inside the Sunda Strait. Full and open symbols correspond to P and T axes respectively. Triangles and diamonds correspond to the graben and Krakatau clusters. Squares show the P and T axis of one event recorded by the worldwide network and which occurred inside the strait. This figure shows that the stress pattern in the vicinity of Krakatau is identical to the stress pattern in the Sunda Strait.

computed from the Krakatau cluster. We propose that the most probable direction of faulting is the one that gives rise to a right lateral fault. Indeed the plane with a direction normal to the Semangko Fault would be a left lateral strike slip which seems difficult to reconcile with the dextral movement of the Semangko fault. So, we propose that this cluster corresponds to a NW-SE dextral strike slip fault. Such a fault, the Batee fault (Figure 1) was described by Karig et al. [1980] north of Sumatra. These faults, transverse to the fore-arc basin probably delineate blocks that rotate along the Semangko fault.

CONCLUSIONS

The analysis of the local seismicity recorded by a microearthquake survey in the Sunda Strait area complemented by bathymetry and data from the worldwide network allow us to draw the following conclusions:

1. Seismic activity in the Sunda Strait area is concentrated in three clusters centered on Krakatau, a graben in the western part of the strait and south of Sumatra. The Krakatau and graben clusters are linked by a fault striking N50°E-N60°E.

2. Our results confirm that the Sunda Strait area is under an extensional tectonic regime. The stress tensor analysis gives a N130°E direction of extension, that is parallel to the

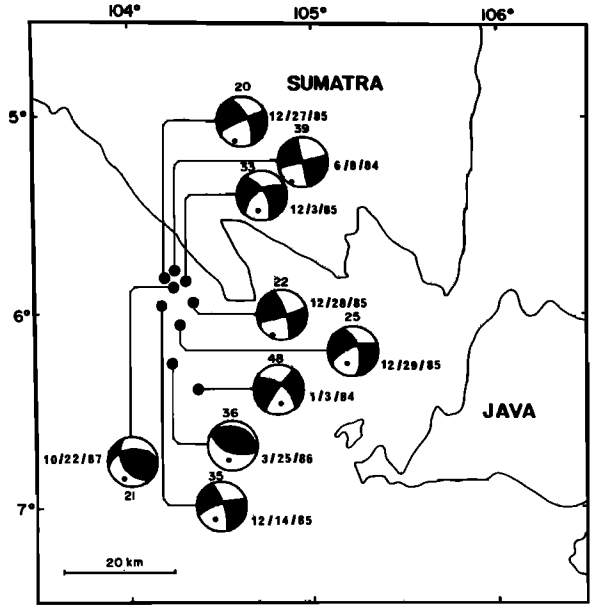

Fig. 14. Harvard centroid moment tensor solutions (CMTS) for the cluster south of Sumatra [e.g. Dziewonski et al., 1989]. Numbers give the depth (in km).

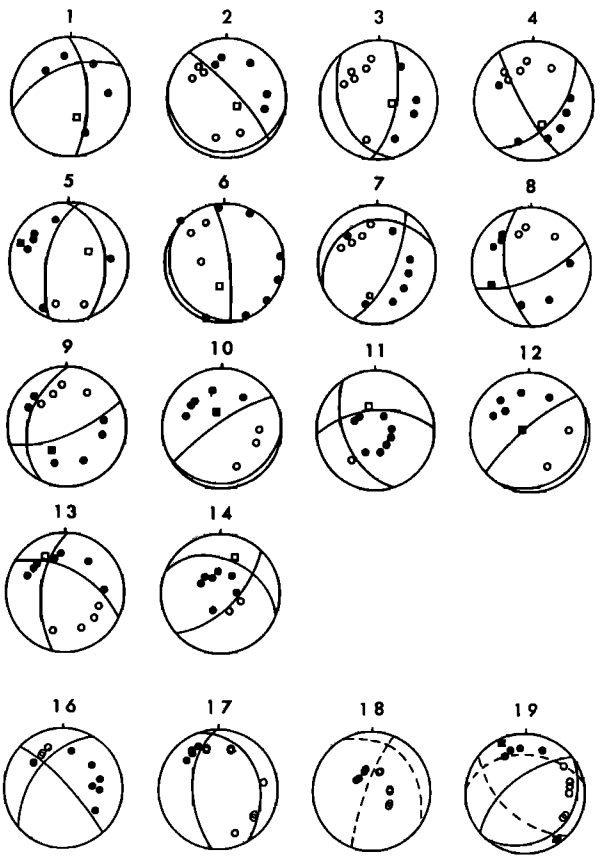

Fig. A1. Lower hemisphere equal area fault plane solution as shown in Figures 9 and 12. Compressional and dilatational first motions are shown as full and open circles respectively. The squares represent the direct waves and dots the refracted waves.

Semangko fault. This crustal stretching should be a result of the NW movement of the Sumatra fore-arc plate (sliver plate) [Huchon and Le Pichon, 1984; Jarrard, 1986]. This result agrees with other geophysical data such as seismic reflection [Lassal et al., 1989].

3. Seismicity south of Sumatra is interpreted as a fault transverse to the fore arc basin. But, obviously, an additional survey which would also involve ocean bottom seismographs is necessary in order to better constrain that seismicity.

4. As a consequence of the crustal extension, the Sunda Strait is characterized by important volcanic activity as shown by large deposits of Quaternary material [Nishimura et al., 1986]. The fact that Krakatau differs from volcanoes common elsewhere in Indonesia can be related to the specific, extensional, tectonic setting. The existence of the presently active Anak Krakatau also appears as a consequence of its location as the intersection of an active fault with the volcanic line running from Panaitan to Rajabasa.

5. Seismicity beneath the Krakatau complex is controlled by the regional stress field but we find a variation with depth that we relate to local effects.

Acknowledgments. We dedicate this work to Jean Bloyet, who enthusiastically participated in the field work and the preliminary interpretations. We thank M. Régnier (ORSTOM), C. Jouannic (ORSTOM), I. Suhardi (BPPT), and S. Wirasantosa and M. E. Arsadi from Puslitbang, Geoteknologi-LIPI for their assistance during the survey and in arranging the field work. We also thank the technician group of Puslitbang Geoteknologi-LIPI (A. Sanyoto, D. Rahayu, Suyatno, Y. Sudrajat, E. Junaidi, D. Rusmana, Jusuf, Eman D. Ruswandi, A. Tatang and Sardiman) for their help in operating the seismographs and thank the people of the area of the survey and the telecommunication stations of Tanjung Karang and Cilegon, Krakatau Observatory in Pasauran and PPA Ujung Kulon. We acknowledge D. Hatzfeld, who supplied us five MEQ instruments and the Volcanological Survey of Indonesia (VSI) and the Indonesian Meteorology and Geophysical Agency (BMG) for providing data of KRK and KLI. We thank E. Carey-Gailhardis for discussions and for providing a program for tensor analysis. The manuscript benefited of discussions with C. Deplus, J. Deverchère, O. Lassal, P. Tucholka and from extensive and detailed reviews by H. Lyon-Caen and D. Hatzfeld. Figure 14 was drawn after original figures produced at I.P.G. Paris using a software program of G. Ekström. This work was suported by A.T.P. "Géologie et Géophysique des Océans" of C.N.R.S, IFREMER, ORSTOM, LIPI (Indonesian Institute of Sciences) and BPP. Teknologi (Agency for the Assessment and Application of Technology).

REFERENCES

Beck, Jr., M.E., On the mechanism of tectonic transport in zones of oblique subduction, *Tectonophysics, 93*, 1-11, 1983.

Camus, G., and P. Vincent, Un siècle pour comprendre l'éruption du Krakatao, *La Recherche, 149*, 1452-1457, 1983.

Camus, G., A. Gourgaud, and P.M. Vincent, Petrologic evolution of Krakatau (Indonesia): Implication for a future activity, *J. Volcanol. Geotherm. Res., 33*, 299-316, 1987.

Carey-Gailhardis, E. and J.L. Mercier, A numerical method for determining the state of stress using focal mechanisms of earthquake populations: Aplication to Tibetan teleseisms and microseismicity of Southern Peru, *Earth Planet. Sci. Lett., 82*, 165-179, 1987.

Deplus, C., Comportement mécanique de la lithosphère océanique: Cas d'une subduction complexe, Ph.D. thesis, Université de Paris Sud, Orsay, 1987.

Diament, M., C. Deplus., M. Larue., P. Tucholka, H. Harjono, P.Kimpouni, C. Mercier, G. Okemba and J.-P. Quetier, Seasat altimetry, marine gravity and magnetism between Java and Sumatra, in *Proceedings Indonesia-France Seminar on Sunda Strait*, pp. 35-44, BPPT, Jakarta, 1987.

Dziewonski, A. M., G. Ekström, J.H. Woodhouse and G. Zwart, Centroid-moment tensor solutions for October-December 1988, *Phys. Earth Planet. Inter., 57*, 179-191, 1989.

Fatwan, S., Pendugaan lapisan bawah tanah permukaan dengan metoda seismik bias di daerah Selat Sunda, S1 Thesis, Institut Teknologi Bandung, 1983.

Fitch, T.J., Plate convergence, transcurrent faults, and internal deformation adjacent to Southeast Asia and western Pacific, *J. Geophys. Res., 77*, 4432-4460, 1972.

Fitch, T.J. and P. Molnar, Focal mechanisms along inclined earthquake zones in the Indonesian-Philippine region, *J. Geophys. Res., 75*, 1431-1444, 1970.

Hamilton, W., Earthquake map of the Indonesian region, *U.S. Geol. Surv. Misc. Inv. Ser. Map I-875-C*, 1974.

Hamilton, W., Tectonics of the Indonesian region, *U.S. Geol. Surv. Prof. Pap., 1078*, 345 pp., 1979.

Hatzfeld, D., S.W. Roecker, J. Nabelek and B. Tucker, Seismicity in the Garm region of Central Asia: Deformation in a zone of continental convergence, *Ann. Geophys., 4B*, 555-566, 1986.

Hatzfeld, D., A.A. Christodoulou, E.M. Scordilis, D. Panagiotopoulos, and P.M. Hatzidimitriou, A microearthquake study of the Mygdonian graben (northern Greece), *Earth Planet. Sci. Lett., 81*, 379-396, 1987.

Huchon, P., and X. Le Pichon, Sunda Strait and Central Sumatra Fault, *Geology, 12*, 668-672, 1984.

Jarrard, R.D., Relations among subduction parameter, *Rev. Geophys., 24*, 217-284, 1986.

Karig, D.E., M.B. Lawrence, G.F. Moore and J.R. Curray, Structural framework of the fore-arc basin, NW Sumatra, *J. Geol. Soc. London, 137*, 1-15, 1980.

Katili, J.A., and F. Hehuwat, On the occurrence of large transcurrent faults in Sumatra, Indonesia, *J. Geosci. Osaka City Univ., 10*, 1-17, 1967.

Kieckhefer, R.M., Geophysical studies of the oblique subduction zone in Sumatra, Ph.D Thesis, 119 pp., Univ. of Calif., San Diego, 1980.

Kiratzi, A.A., E.E. Papadimitriou, and B.C. Papazachos, A microearthquake survey in the Steno dam site in northwestern Greece. *Ann. Geophys., 5B*, 191-166, 1986.

Klein, F.W., Hypocenter Location Program: Hypoinverse, *U.S. Geol. Surv., Open File Rep., 78-694*, 113 pp., 1978.

Lassal, O., P. Huchon and H. Harjono, Extension crustale dans le détroit de la Sonde (Indonésie): Données de la sismique réflexion (Campagne Krakatau), *C. R. Acad. Sci., Ser. 2, 309,*, 205-212, 1989.

McCaffrey, R., P. Molnar, and S.W. Roecker, Microearthquake seismicity and fault plane solution related to arc-continent collision in the eastern Sunda arc, Indonesia, *J. Geophys. Res, 90*, 4511-4528, 1985.

Minikami, T., Seismology of volcanoes in Japan, in *Physical Volcanology*, edited by L. Civetta, P. Gasparini, G. Luongo and A. Rapolla, pp. 1-27, Elsevier, New York, 1974.

Minster, J.B., and T.H. Jordan, Present-day plate motion, *J. Geophys. Res., 83*, 5331-5354, 1978.

Molnar, P. and P. Tapponnier, Cenozoic tectonics of Asia: Effects of continental collision, *Science, 189*, 419-426, 1975.

Newcomb, K.R., and W.R. McCann, Seismic history and seismotectonic of the Sunda Arc, *J. Geophys. Res., 92*, 421-439, 1987.

Ninkovich, D., Late Cenozoic clockwise rotation of Sumatra, *Earth Planet. Sci. Lett., 29*, 269-275, 1976.

Nishimura, S., J. Nishida, T. Yokoyama, and F. Hehuwat, Neo-tectonics of the Strait of Sunda, Indonesia, *J. Southeast Asian Earth Sci, 1*, 81-91, 1986.

Noujaim, A.K., Drilling in a high temperature and overpressured area Sunda Straits, Indonesia, in *Proceedings of Fifh Annual Convention*, pp.211-214, Indonesian Petroleum Association, Jakarta, 1976.

Raitt., R.W., Marine seismic studies of the Indonesian island arc (abstract), *Eos Trans. AGU, 48*, 217, 1967.

Sclater, J.G. and R.L. Fisher, Evolution of the east-central Indian Ocean, with emphasis on the tectonic setting of the Ninety-East Ridge. *Geol. Soc. Am. Bull., 85*, 683-702, 1974.

Soeria-Atmadja, R., R.C.Maury, H. Bougault, J.L. Joron, H. Bellon, and D. Hasanuddin, Présence de tholeiites d'arrière-arc Quarternaires en Indonésie: Les basaltes de Sukadana (Sud de Sumatra) (abstract), in *Réunion des Sciences de la Terre*, Clermont-Ferrand, 1986.

Shimizu, H., S. Ueki, and J. Koyama, A tensile-shear crack model for the mechanism of volcanic earthquakes, *Tectonophysics, 144*, 287-300, 1987.

Tapponnier, P., G. Peltzer, A.Y. Le Dain, R. Armijo, and P. Cobbold, Propagating extrusion tectonics in Asia: New insights from simple experiments with plasticine, *Geology, 10*, 611-616, 1982.

Untung, M. and Y. Sato, *Gravity and Geological Studies in Java*, Geoligical Survey of Indonesia and Geological Survey of Japan, 207 pp., 1978.

Van Bemmelen, R.W., *The Geology of Indonesia*, Government Printing Office, The Hague, 732 pp., 1949.

Zen, M.T., Krakatau and the tectonic importance of Straits of Sunda, *Bul. Jurusan Geol., 12*, 9-22, 1983.

M. Diament, J. Dubois, H. Harjono and M. Larue, Laboratoire de Géophysique (URA du CNRS 1369), Bât. 509, Université Paris Sud, 91405 Orsay-Cedex, France.

M.T. Zen, Laboratorium Geofisika, Jurasan Geologi, Institut Teknologi Bandung, Jl. Ganesha 10, Bandung 40132, Indonesia.

(Received November 17, 1988;
revised January 24, 1990;
accepted January 25, 1990.)